IOP Conf. Series: Materials Science and Engineering **174** (2017) 012005 doi:10.1088/1757-899X/174/1/012005

Influence of tooth profile on the noncircular gear tooth contact

A Cristescu, L Andrei and B Cristescu

Department of Mechanical Engineering, "Dunărea de Jos" University of Galaţi, Domneasca 47, Romania

E-mail: landrei@ugal.ro

Abstract. With noncircular gears, the continuous modification of the tooth meshing, in terms of variation of the tooth profiles and the line of action position and inclination, makes difficult the implementation of a general standard procedure for the analysis of the noncircular gears tooth contact. In this paper, the authors present a graphical approach that enables the tooth contact static pattern to be produced and evaluated in case of a noncircular gear with complex geometry of the pitch curve. The study is virtually developed, in AutoCAD environment, by animating and investigating the gear solid models in mesh. The tooth static contact analysis enables the path of contact area and distribution to be evaluated in correlation with the following variable initial data: gear pitch curve geometry, tooth profile geometry, as a consequence of different generating procedures, and the gear pressure angle. It was found out that the noncircular gear tooth contact could be improved by choosing different procedures for the tooth flank generation in concave and convex zones and by increasing the gear pressure angle.

1. Introduction

The design of the circular gears is controlled through specific standardized calculation. By comparison, the design of the noncircular gears is a complex process based on two main steps: (i) noncircular centrodes modelling and (ii) teeth generation. Considering the design input data, the approaches to noncircular centrodes modeling are mainly based on the transmission ratio variation [1 - 3], the law of motion for the driven element [4] or the driving centrode geometry [5, 6]. The teeth generation is developed from either analytical procedures that consider the particularities of gear line of action [7, 8], the traditional theory of the enveloping surfaces [9, 10], or from the simulation of the gear generation [11, 12]. Basically, the noncircular gears teeth generation methods presented by specialists are based on a constant pressure angle of a the standard value of 20°, but there are certain researches who, in order to improve the meshing conditions, consider different values of the pressure angle: either for all the teeth [11] or from one tooth to another [13, 14].

While the circular gears meshing process is well known and controlled, due to the variable and complex geometry of the noncircular gears, their meshing exhibits specific behavior which is difficult to predict. Unlike the circular gears meshing as approached by standardized procedures and calculations, the teeth contact analysis for the noncircular gears is developed through experimental methods based both on specific elements of the standard gear geometry and on virtually developed models of the noncircular gears [15 - 17].

The authors of this paper have developed a graphical procedure to analyze the static noncircular gear contact by taking into account the characteristics of the noncircular gears meshing process, i.e. the variable position of the instantaneous contact point of the mating centrodes along the gears center line and the variable inclination of the line of action that is related, by a constant pressure angle, to the common tangent of the conjugate noncircular centrodes. All the required rolling parameters are calculated by Hypertext Preprocessor (PHP) codes and imported into the AutoCAD environment. The centrodes geometry is automatically investigated and the teeth placed on convex and concave zones, with minimum and maximum curvature, are picked up. An analytical procedure for the gear teeth profiles generation will provide the best accuracy for all the geometrical and dimensional tooth parameters required by further investigations on gears performance. The virtual gears are built up combining PHP calculus and computer graphics operations specific to the AutoCAD. Finally, the virtual solid gears models are manipulated to simulate the gears meshing and to produce the teeth contact patterns. The distribution and area of the contact pattern are analyzed in correlation with the variable gears design data such as tooth profile geometry provided by the generation process and the gear pressure angle.

2. Noncircular gear teeth generation

In order to generate noncircular gear teeth, the specific kinematics of the rolling of the rack-cutter over the noncircular gear blank is considered. To enable generation of noncircular gears with complex geometries, that exhibit also concave zones, without any undercutting, a single tooth rack-cutter of standard geometry is considered. Each flank generating process is locally analyzed in the proximity of the intersection point E_i between the current tooth flank and the gear noncircular pitch curve (figures 1, 2). The analytical procedure of the tooth flank generation process consists in expressing the intersection point between the rack cutter tooth flank and the current line of action during the rolling motion and is presented in detail in previous publications [17, 18]. As the main objective of the paper is to analyze the influence of the noncircular gear tooth geometry on the tooth contact pattern, variations in tooth geometry are achieved by taken into account the following hypotheses: (I) the tooth flank generation is developed by the pure rolling of the rack cutter on both the noncircular pitch curve and on the local osculating circle; (II) the tooth flank generation is developed by the pure rolling of the rack cutter on the noncircular gear pitch curve, considering the pressure angle at different values.

2.1. Using rolling on the noncircular pitch curve

The first hypothesis of generating the noncircular gear tooth flanks considers the rolling motion of the rack cutter tooth on the correct gear pitch curve. Figure 1 illustrates the geometry and the dimensional parameters taken into account while generating the tooth operating flank addendum, showing:

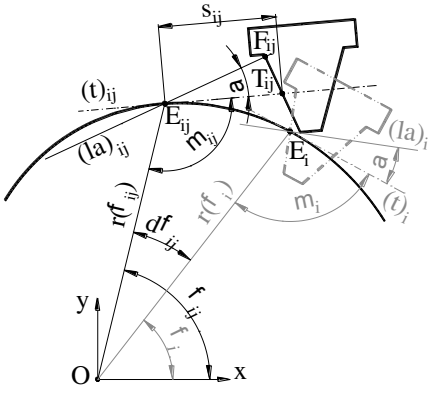

Figure 1. Geometric and kinematics of tooth flank generation using rolling on the noncircular pitch curve.

(i) the starting position of the rack cutter tooth and its orientation specific to point E_i. The rack cutter pitch line is aligned to the local tangent $(t)_i$ that is inclined by μ_i angle, relative to the current radius $r(\varphi_i)$. The first point of the tooth flank profile is $F_i \equiv E_i$;

(ii) an arbitrary position of the rack cutter tooth, after the rolling motion defined by the rotational angle $d\varphi_{ij}$ and the displacement s_{ij} equal to the length of the noncircular arc E_iE_{ij}; the rack cutter is firstly rotated about E_{ij}, so that its pitch line is aligned to the current tangent $(t)_{ij}$ to the noncircular centrode, and is translated by the rolling distance. The generated point F_{ij} of the tooth flank is picked up at the intersection between the rack cutter tooth operating flank and the current line of action $(la)_{ij}$ that is inclined by the constant pressure angle α with respect to $(t)_{ij}$ line. Analyzing the generating process geometry and kinematics from figure 1, the tooth operating flank for the addendum zone is described by the equations:

$$\begin{aligned} x_{ij} &= r(\varphi_{ij}) \cdot \cos\varphi_{ij} - s_{ij} \cdot \cos\alpha \cdot \cos(\mu_{ij} + \alpha + \varphi_{ij}), \\ y_{ij} &= r(\varphi_{ij}) \cdot \sin\varphi_{ij} - s_{ij} \cdot \cos\alpha \cdot \sin(\mu_{ij} + \alpha + \varphi_{ij}) \end{aligned} \tag{1}$$

where φ_{ij} and $r(\varphi_{ij})$ are the polar coordinates of the instantaneous center of rotation E_{ij}, s_{ij} - the rack displacement during the rolling motion, μ_{ij} - the inclination angle of the tangent $(t)_{ij}$ with respect to the current radius, α - the constant pressure angle.

Similar equations are written for the tooth dedendum profile of the operating flank and for the non-operating flanks, considering the proper rolling and rack cutter flank [17, 18].

2.2. Using rolling on the local osculating circle

Analyzing the generating process geometry and kinematics from figure 2, when the rolling motion is performed relative to the local osculating circle, specific to point E_i, the tooth operating flank for the addendum zone is described by equations:

$$\begin{aligned} x_{ij} &= r(\varphi_i) \cdot \cos\varphi_i - s'_{ij} \cdot \cos\alpha \cdot \cos(\mu_i + \alpha + \varphi_i), \\ y_{ij} &= r(\varphi_i) \cdot \sin\varphi_i - s'_{ij} \cdot \cos\alpha \cdot \sin(\mu_i + \alpha + \varphi_i) \end{aligned} \tag{2}$$

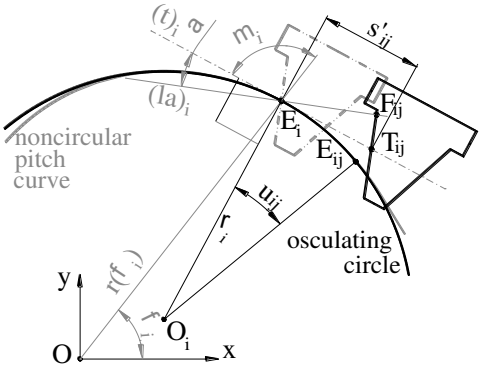

Figure 2. Geometric and kinematics of tooth flank generation using rolling on the local osculating circle**.**

where φ_i and $r(\varphi_i)$ are the polar coordinates of the instantaneous center of rotation E_i, s'_{ij} - the rack displacement along the tangent $(t)_i$, μ_i - the inclination angle of the rack cutter pitch line with respect to the radius $r(\varphi_i)$. The rack cutter displacement, s'_{ij}, is calculated by:

$$s'_{ij} = \rho_i \cdot u_{ij} \tag{3}$$

where ρ_i is the local osculating circle radius, u_{ij} – the incremental rotational angle of the rolling process relative to the osculating circle.

The tooth dedendum profile of the operating flank and the non-operating flank are described by similar equations [18].

For a pair of noncircular gears defined by the transmission ratio $m_{21}(\varphi)$ and the gear center distance D, considering the gears meshing and the coordinate transformation operations, the tooth flanks for the mating noncircular gears are also analitically described [17]. The original PHP codes enable the teeth flanks profiles generation for the noncircular gears pairs. To complete the gear representations, the numerical data is imported to AutoCAD environment and editing operations are applied.

3. Tooth contact analysis

The gears static tooth contact is computed based on a simple geometric approach that are using the noncircular gears solid models and the AutoCAD facilities, as presented in other previous publications [19, 20]. The tooth contact pattern is considered as the composed solid that results by intersecting the main and adjacent pairs of meshing teeth whose elastic deformations were not taken into account. The static analysis refers to the gears unload simulating meshing, although an initial extremely reduced torque and rotation, respectively, should be applied to the pinion in order to enable the solids intersection. The paper aim is just to compare the teeth meshing for the above two gear teeth geometries induced by the generation method; a comparison with standard gears meshing is difficult to be made while the tooth flank geometry differs to one tooth to another, there is a different module that defines the tooth geometry along the noncircular gear pitch curves etc., but the authors would consider it for further researches.

Investigations on the noncircular gears static contact is particularly developed for a gears train that is defined by the following design data: gear center distance D = 200 mm, gears number of teeth z_1 = z_2 = 36, gear facewidth is B = 20 mm, pressure angle $\alpha \in \{15°, 20°, 25°\}$, tooth position chosen so that a constant angular pitch is met ($\varphi_i = i \cdot 2\pi/z_1$, where $i = 0...(z_1 - 1)$) and the gear transmission ratio is defined by:

$$m_{21}(\varphi) = 1 + \frac{1}{4} \cdot \cos\varphi + \frac{1}{3} \cdot \sin 3\varphi \tag{4}$$

The gear transmission ratio is chosen so as complex pitch curve geometries are achieved, that exhibit convex, concave and almost linear zones. Two pairs of teeth chosen for the analysis (figure 3) are placed in the convex zone, with the highest radius of curvature (tooth D_{33}) and in the concave zone, with the smallest radius of curvature (tooth D_{22}).

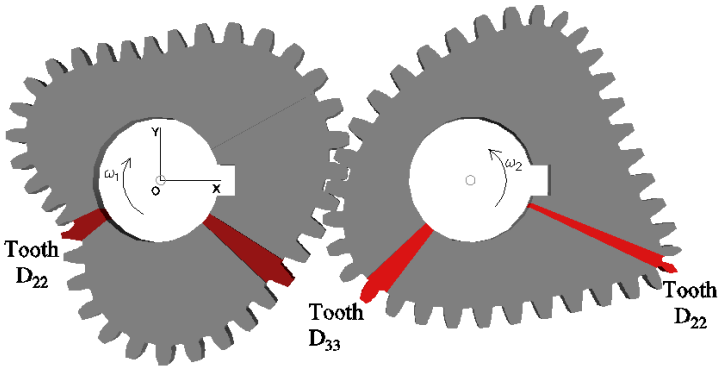

Figure 3. Virtual solid models of noncircular gears.

The algorithm proposed for the tooth contact pattern investigation consists of (figure 4):

Step1: The gear teeth being analyzed are selected and identified by positioning and geometrical parameters. The main tooth and other four teeth are taken into account (figure 4a);

Step2: The tooth being analyzed is placed on the center line by a proper rotational angle of pinion (φ_1) and driven gear (φ_2), respectively. To produce the contact pattern, the static meshing is considered and a minimum torque is applied, which is further reflected by a controlled interference induced by an initial pinion rotational angle of 0.005° (figure 4b);

Step3: Incremental rolling by $\Delta\varphi_1 = 1^{\circ}$ is applied in both counter clock and clockwise in order to highlight the tooth contact during all the meshing of the conjugated teeth (figure 4c);

Step4: The solids are intersected to obtain the static path of contact for the controlled interference. The tooth contact pattern distribution is illustrated on the driving gear teeth (figure 4d) and its area is measured along the main tooth and on the other teeth engaged in the mesh.

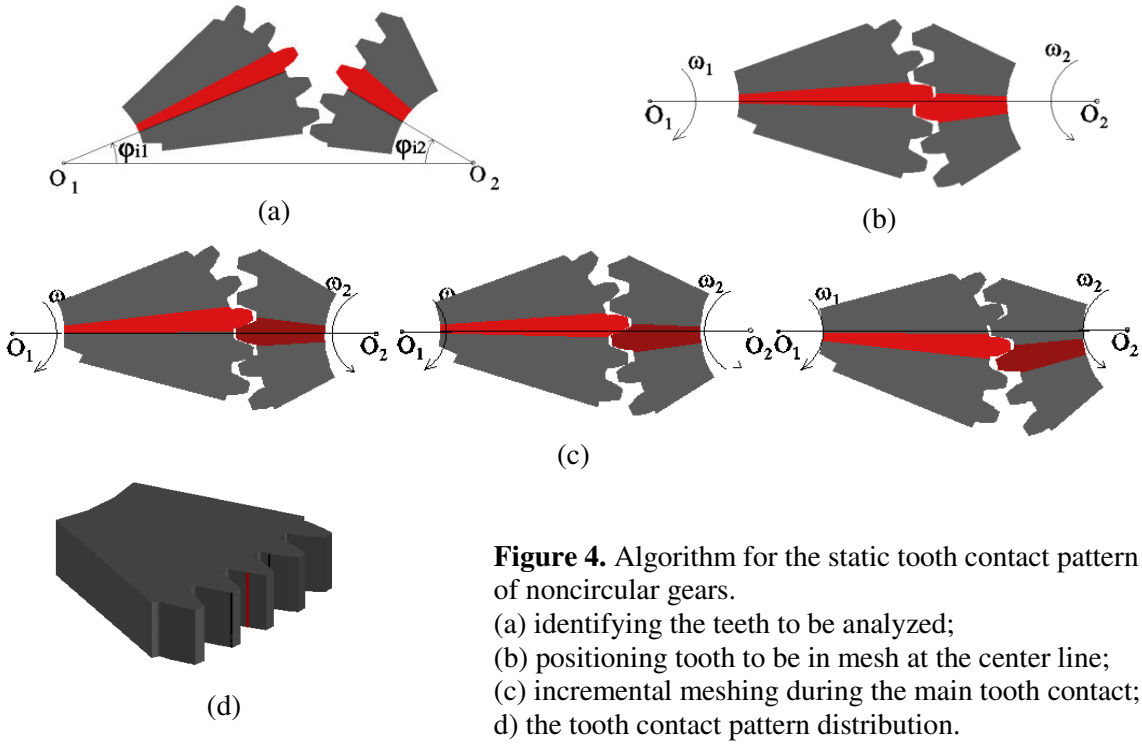

Figure 4. Algorithm for the static tooth contact pattern of noncircular gears.
(a) identifying the teeth to be analyzed;
(b) positioning tooth to be in mesh at the center line;
(c) incremental meshing during the main tooth contact;
d) the tooth contact pattern distribution.

3.1. Influence of tooth generation process on the static tooth contact pattern
Figure 5 illustrates details of the selected teeth geometry of the noncircular driving gear generated by the rack cutter rolling on the noncircular pitch curve (named as AnCG20) and on the local osculating circle (AnAG20), respectively. The study of the static contact pattern of the selected pairs of teeth, for both noncircular gears trains, provides data regarding the number of teeth in mesh, the area of the path of contact on the main analyzed tooth (APT), the value of the total contact area (APG) and the value of the gear rotational angle while the analyzed tooth is in mesh.

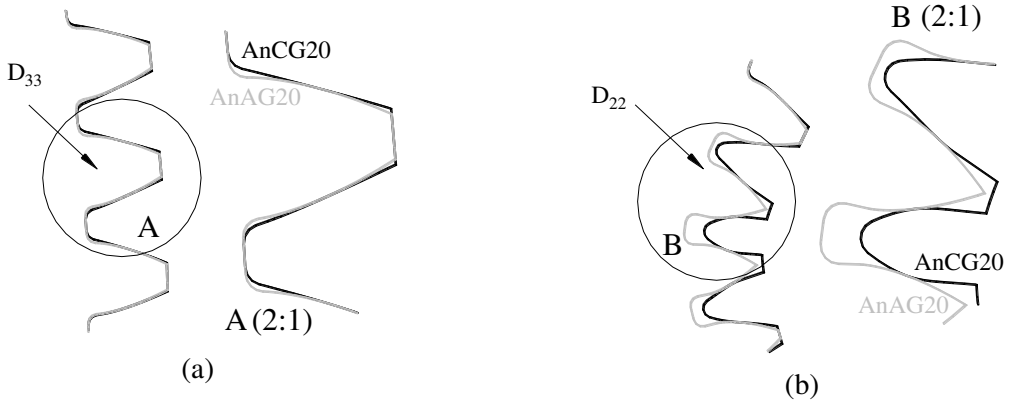

Figure 5. Details of noncircular driving gear generated by accurate (AnCG20) and approximate (AnAG20) generation process on convex zone, with the highest curvature radius (a) and on concave zone, with the smallest curvature radius (b).

Table 1 and figure 6 present a selection of data recorded while the specified teeth are in mesh. The global area of contact (APG), presented in table 1, is the sum of the total areas of the solids that result by intersecting the main teeth and the adjacent pairs of meshing teeth; the tooth contact area (APT), shown in figure 6, is the total area of the solid that results by intersecting the main teeth (D_{33}, D_{22}, respectively). It is noticed that for both gear trains, the teeth D_{33} and D_{22} are in mesh while the driving gear is rotated by 15° and 14°, respectively. Comparing the total area of contact (APG) in the selected convex zone, decreases in the area are recorded in case of ANAG20, by 25% while tooth D 33 gets into mesh, by 59% when contact occurs on the gears center line and by 15% when tooth gets out of mesh. This could be explained by the higher curvature of the correct tooth flank due to the rolling on the noncircular pitch curve arc whose curvature decreases in the vicinity of teeth D_{33}, while the approximate tooth flank is an involute of a circular arc with constant high radius, almost a rectilinear segment. The analysis of the tooth contact pattern in the vicinity of tooth D_{22} shows a slightly better behavior for the concave zones of the AnAG20 gear compared to the accurately generated gears, the total contact area being increased by 9% when tooth D_{22} gets into mesh, by 8.2% at center line and by 9.6% when tooth gets out of the mesh. In particular, the comparison of the D_{22} tooth contact pattern area is illustrated in figure 6.

Table 1. Contact parameters for noncircular gears generated by accurate and approximate rolling.

Tooth		D_{33}	D_{33}	D_{33}	D_{22}	D_{22}	D_{22}
Tooth position		Gets into mesh	On center line	Out of mesh	Gets into mesh	On center line	Out of mesh
AnCG20	No.of teeth	3	3	3	2	3	3
	APG [mm^2]	393.494	435.432	212.065	99.644	351.419	184.228
AnAG20	No.of teeth	2	3	3	2	3	3
	APG [mm^2]	295.183	179.988	179.079	108.815	380.354	201.912

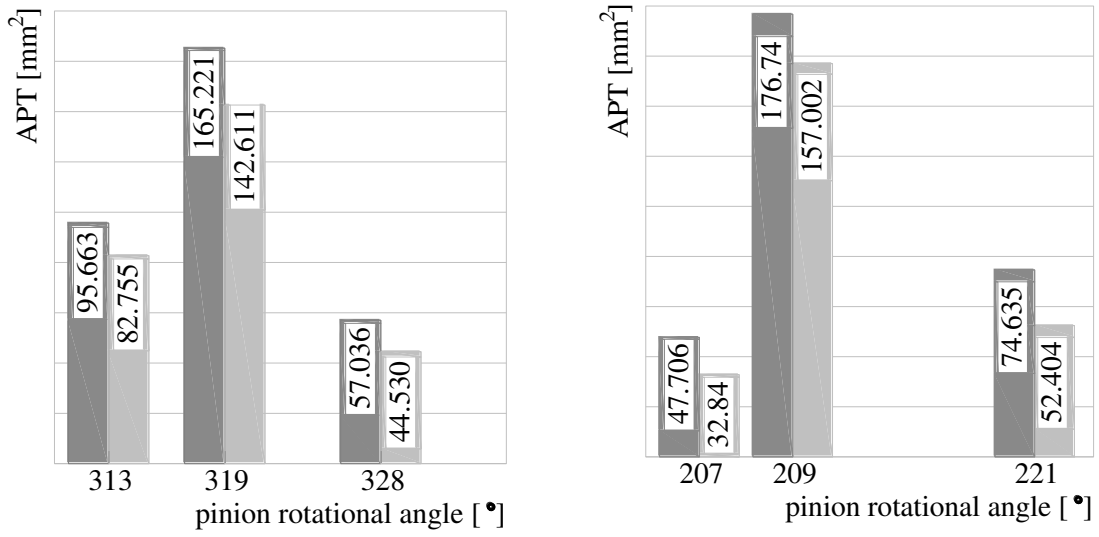

(a) (b)

Figure 6. Contact area on teeth D33 (a) and D_{22} (b), for the AnCG20 and AnAG20 gear trains.

3.2. Influence of pressure angle on the static tooth contact pattern

To analyze the influence of the pressure angle on the tooth contact pattern, three gear trains are compared, generated by using an accurate rolling process, making use of the above mentioned gears

design data and three values of the pressure angle, resulting the AnCG15 gear pair for α = 15°, the AnCG20 gear pair for α = 20° and the AnCG25 gear pair for α = 25°, respectively (figure 7).

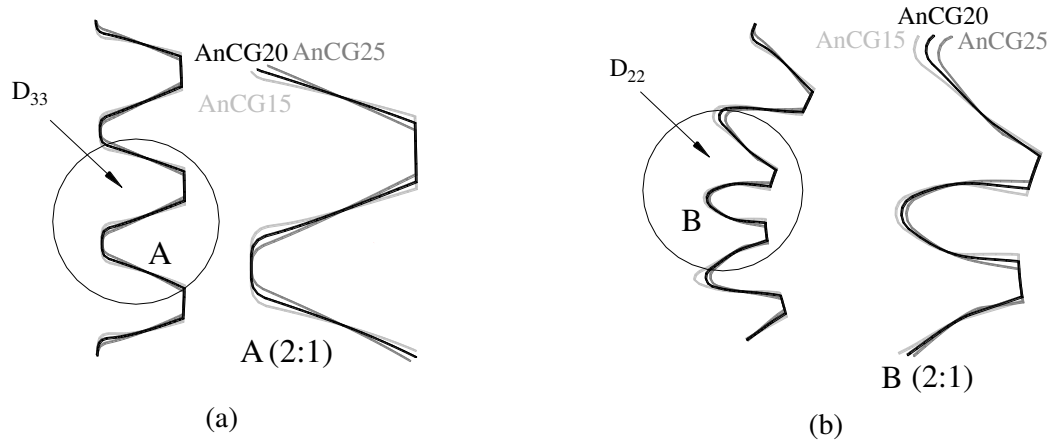

Figure 7. Details of noncircular driving gear generated using α = 15° (AnCG15), α = 20° (AnCG20) and α = 25° (AnCG25) for convex zone, with the highest curvature radius (a) and for concave zone, with the smallest curvature radius (b).

Table 2. Contact parameters for noncircular gears designed with variable pressure angle.

Tooth		D_{33}	D_{33}	D_{33}	D_{22}	D_{22}	D_{22}
Tooth position		Gets into mesh	On center line	Out of mesh	Gets into mesh	On center line	Out of mesh
AnCG20	No.of teeth	3	3	3	2	3	3
	APG [mm^2]	393.494	435.432	212.065	99.644	351.419	184.228
AnCG15	No.of teeth	3	3	2	2	3	3
	APG [mm^2]	312.494	402.714	198.451	99.644	351.419	184.228
AnCG25	No.of teeth	3	3	2	2	3	3
	APG [mm^2]	398.205	448.032	230.119	118.004	398.212	231.509

The pressure angle influence on the static contact conditions is determined by analyzing the data from table 2 and figure 8. It appears that for both the convex and concave areas, greater pressure angle values determine improved meshing conditions by increasing the contact area for the tooth contact pattern. Thus, for tooth D_{33}, the average area is with 9.79% higher for AnCG20 than the average area for gear trainAnCG15 and with 10.26% lower than the values recorded for AnCG25 (table 2). Similarly, for tooth D_{22}, the growth in the average area of the contact path is 14.03% when comparing the AnCG20 and AnCG15 gear trains and 12.60% for AnCG25 to AnCG15 (figure 8).

4. Conclusions

Conditions of noncircular gear trains meshing are studied in terms of tooth static contact pattern. A virtual graphical method is developed in order to produce the tooth contact and to enable analysis of the influence of the gear generation method and pressure angle, respectively, on the meshing characteristics. The analysis is focused on the contact of the teeth situated in convex and concave zones of the noncircular gears, with extreme values of the gear pitch curve radius of curvature.

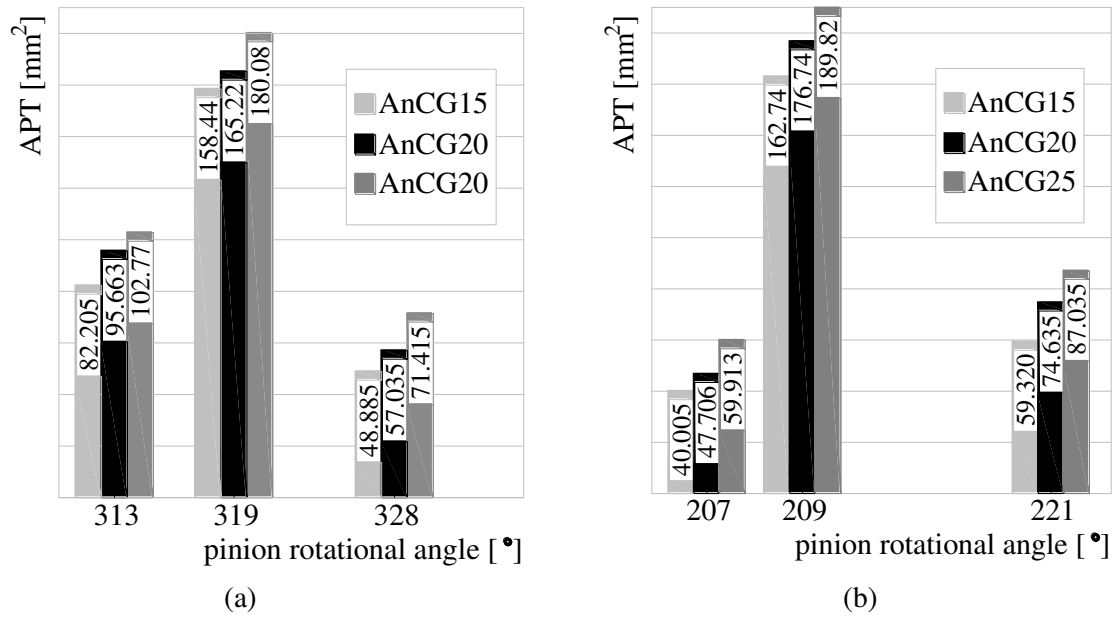

Figure 8. Contact area on teetth D_{33} (a) and D_{22} (b) measured on the AnCG15, AnCG20 and AnCG25 gear trains.

Original PHP codes provide neccessary data base to generate the noncircular mating centrodes and the teeth flanks profiles that are further imported in AutoCAD environment where the virtual solid models of the gear trains are produced and incrementally got into the mesh. The teeth contact pattern size and distribution are investigated and compared for noncircular gear trains with variable tooth flank geometries, generated while the rach cutter is rolling on the correct noncircular pitch curve and on the local osculating circle, approximating the tooth profile by an involute. It appeared that gears accurately generated, by performing the rolling process over the noncircular pitch curve, led to better meshing characteristics in case of convex zones, compared to gears generated by rolling over local osculating circle, the contact area of which was improved into concave zones, with high curvature. Modifying the gear tooth geometry by varying the gear pressure angle, it was noticed that high pressure angle provided, for both the convex and concave zones, improved meshing conditions.

Acknowledgements
The work has been funded by the Sectorial Operational Programme Human Resources Development 2007-2013 of the Ministry of European Funds through the Financial Agreement POSDRU/159/1.5/S/132397.

References
[1] Tsay M F and Fong Z H 2005 Study on the generalized mathematical model of noncircular gears *Math. Comp. Model.* **41** 555–569
[2] Mundo D 2006 Geometric design of a planetary gear train with non-circular gears *Mech. Mach. Theory* **41** 456–472
[3] Cristescu A, Cristescu B and Andrei L 2014 Generalization of Multispeed Gear Pitch Curves Design *Appl. Mech. Mater.* **659** 559–564
[4] Laczik B 2007 Design and Manufacturing of Non-Circular Gears by Given Transfer Function *Proc. ICT* 101–109
[5] Bair B W, Chen C F, Chen S F and Chou C Y 2007 Mathematical Model and Characteristic Analysis of Elliptical Gears Manufactured by Circular-Arc Shaper Cutters *J. Mech. Design* **129** 210-214

[6] Vasie M and Andrei L 2012 Design and generation of noncircular gears with convex-concave pitch curves *The Annals of "Dunarea Jos" University of Galati, Mathematics, Physics, Theoretical Mechanics* 55–60
[7] Danieli A, Mundo D 2005 New developments in variable radius gears using constant pressure angle teeth *Mech.Mach Theory* **40** 203-217
[8] Gao S, Igarashi S, Takayama F, Ohomote R, Tang X, Chen X and Li J 2006 Design and analysis of shapes of elliptic gears *12th Int. Conf. on Geometry and Graphics*
[9] Litvin F L 2009 *Noncircular Gears Design and Generation* (Cambridge University Press)
[10] Figliolini G and Rea P 2014 Effects of the design parameters of involute gears generated by rack-cutters *International Gear Conference 2014: 26th–28th August 2014, Lyon* pp 294-302
[11] Li J, Wu X and Mao S 2007 Numerical computing method of noncircular gear tooth profiles generated by shaper cutters *The International Journal of Advanced Manufacturing Technologies* **33** 1098–1105
[12] Vasie M and Andrei L 2011 Noncircular gear design and generation by rack cutter *The Annals of "Dunarea Jos" University of Galati, Mathematics, Physics, Theoretical Mechanics* **1** 81–86
[13] Kitano A 1977 Elliptic gear wheel *United States Patent 4036073A*
[14] Danieli G A 2007 Toward a greater industrial application of variable radius gearing *12th IFToMM World Congress*
[15] Khan S 2015 Simulation and analysis of transmission error in helical non circular gear model *Int. International Journal of Mechanical Engineering and Technology* **6** 128–136
[16] Barkah D, Shafiq B and Dooner D 2000 3D Mesh generation for static stress determination in spiral noncircular gears used for torque balancing *J. Mech. Design* **124** 313-321
[17] Cristescu B, Cristescu A and Andrei L 2014 Analytical generation of involute flanks of noncircular gear tooth *The Annals of "Dunărea de Jos" University of Galati, Mathematics, Physics, Theoretical Mechanics* **1** 36-43
[18] Cristescu A, Cristescu B and Andrei L 2015 Finite element analysis of multispeed noncircular gears *Appl. Mech. Mater* **808** 244-251
[19] Andrei L, Andrei G, Walton D and Dean K 2008 Analysis of gear quality criteria and performance of curved face width spur gears *The Annals of "Dunărea de Jos" University of Galaţi*, Fascicle VIII Tribology 30–34
[20] Vasie M and Andrei L 2012 Analysis of noncircular gear meshing *Mechanical Testing and Diagnosis* **4** 70-78